International Journal of Anatomy and Research,
Int J Anat Res 2026, Vol 14(3):9622-35. ISSN 2321-4287
DOI: https://dx.doi.org/10.16965/ijar.2026.178

Original Research Article

Protective Effects of Vitamins A, C, and E on Ovarian Histopathology, Apoptotic Signaling, Oxidative Stress, and Early Embryonic Development in Zinc Oxide Nanoparticle-Induced Toxicity in Female Rats

Sally Adnan Mousa Al-Rikabi

Department of Medical Laboratory Techniques, Kut- Technical Institute, Middle Technical University, Baghdad, Iraq.

ABSTRACT

Background: Zinc oxide nanoparticles (ZnO-NPs) are one of the most common metal oxide nanomaterials produced in the world and their uses are increasing in cosmetics, food packaging, sunscreens and in pharmaceuticals as well as agrochemicals. There is increasing concern on their possible reproductive toxicity, especially on ovarian tissue in females.

Aims: To investigate the role of oral co-delivery of vitamins A, C, and E (alone and in combination) in reducing ZnO-NP-induced ovarian oxidative damage, histopathological destruction, apoptotic activation, hormonal perturbation, and impaired early embryonic development in adult female Wistar rats.

Methods: Forty-eight adult female Wistar rats (10–12 weeks, 180–220 g) were randomized into six equal groups (n = 8) and treated by oral gavage for 28 days: G1 (saline control), G2 (ZnO-NP 100 mg/kg), G3–G5 (ZnO-NP + vitamin A [1000 IU/kg], C [200 mg/kg], or E [100 mg/kg]), and G6 (ZnO-NP + combined A+C+E). On the 5th gestational day (GD 5) after mating, animals were sacrificed. Assays comprised ovarian oxidative stress biomarkers (MDA, GSH, SOD, CAT), serum reproductive hormones (FSH, LH, estradiol, progesterone), haematoxylin and eosin (H&E) histopathology with semi-quantitative lesion scoring, immunohistochemistry (IHC) of Bax, Bcl-2

Results: ZnO-NP exposure resulted in a high level of lipid peroxidation, antioxidant depletion, follicular atresia, vascular congestion, stromal edema, inflammatory infiltration, a 61-fold increase in ovarian Bax/Bcl-2 ratio (0.10 All the vitamins partially reversed these changes; the A+C+E combination produced the overall most protection with all parameters returning to statistically equal levels of controls.

Conclusion: ZnO-NPs cause multi-level reproductive toxicity by activating the intrinsic apoptotic pathway by oxidative stress in granulosa cells. Combinations of antioxidant vitamin supplements have comprehensive, synergistic effects and should be the subject of additional translational research.

KEYWORDS: zinc oxide nanoparticles; ovarian toxicity; histopathology; apoptosis; Bax; Bcl-2; caspase-3; TUNEL; oxidative stress; vitamin A; vitamin C; vitamin E; follicular atresia; early embryonic development; female rats.

Corresponding Author: Dr. Sally Adnan Mousa Al-Rikabi, Department of Medical Laboratory Techniques, Kut- Technical Institute, Middle Technical University, Baghdad, Iraq.
E-Mail: sally.adnan@mtu.edu.iq

Access this Article online	Journal Information
Quick Response code	**International Journal of Anatomy and Research** ISSN (E) 2321-4287 | ISSN (P) 2321-8967 **https://www.ijmhr.org/ijar.htm** **DOI-Prefix:** https://dx.doi.org/10.16965/ijar
DOI: 10.16965/ijar.2026.178	**Article Information**
	Received: 09 May 2026 Accepted: 15 Jul 2026 Peer Review: 13 May 2026 Published (O): 01 Sep 2026 Revised: 10 Jun 2026 Published (P): 05 Sep 2026

INTRODUCTION

Engineered nanomaterials have found their way into numerous industries in the contemporary world and zinc oxide nanoparticles (ZnO-NPs) are some of the most widely manufactured metal oxide nanomaterials on earth. These possess photocatalytic, UV-absorbing, and antimicrobial properties, along

with a favourable biocompatibility profile, which has led to their use in sunscreens, cosmetics, food packaging, biomedical imaging agent formulations, feed additives, and agrochemical formulations [1,2].

This extensive use has simultaneously raised significant concerns about unintended biological impacts after occupational, environmental or dietary exposure.

After oral intake, ZnO-NPs partially dissolve in the acidic gastric environment, releasing free Zn2+ ions, and remaining unabsorbed nanoparticles can cross the intestinal epithelial cell via endocytic and paracellular routes. The resultant systemic distribution leads to accumulation in the most highly perfused, metabolically active organs such as the liver, kidneys, spleen, and the gonads [3-5].

Experimental evidence is on the increase that both the particulate and ionic fraction are capable of causing oxidative stress, mitochondrial dysfunction, genotoxicity and apoptosis in a variety of cell types [6, 7].

The mammalian ovary is especially susceptible to oxidative attacks since folliculogenesis, steroidogenesis, and meiotic maturation require redox signalling that is highly controlled. The overabundance of reactive oxygen species (ROS) interferes with granulosa cell proliferation, quality of oocytes, follicular atresia, and the hypothalamic-pituitary-gonadal (HPG) axis [8-10]. It has been proven by experimental reports that subchronic exposure to ZnO-NPs increases malondialdehyde (MDA), reduces reduced glutathione (GSH), inhibits superoxide dismutase (SOD) and catalase (CAT) as well as causes morphological damage to ovarian follicles [11,12]

At the heart of the pathophysiology of oxidative follicular damage is the activation of the apoptotic cascade in granulosa cells. The balance between pro-apoptotic Bcl-2 family proteins; specifically, Bax, and anti-apoptotic ones; specifically, Bcl-2 regulate the intrinsic (mitochondrial) apoptotic pathway. Bax facilitates mitochondrial outer membrane permeabilization (MOMP), the release of cytochrome c, which triggers caspase-9 and, subsequently, the executioner caspase-3, resulting in internucleosomal DNA fragmentation, which can be detected using the TUNEL assay, under excessive ROS [13-17]; Porter and Jän the ratio of Bax/Bcl-2 expression in ovarian granulosa cells is thus a decisive mechanistic index of the propensity to apoptosis in toxic stress.

Biologically valid possibilities to prevent this redox-mediated damage include classical antioxidant vitamins that mitigate the damage at several pathway levels. Vitamin A (retinol) and its metabolites play a role in stabilizing membranes and cell differentiation of follicular and luteal cells through nuclear retinoic acid receptors [18]. Vitamin C (ascorbic acid) is a strong aqueous phase scavenger of peroxyl and hydroxyl radicals, revitalizes oxidized vitamin E and is enriched in follicular fluid [19-21]. Vitamin E (alpha-tocopherol) selectively breaks lipid-peroxidation-chain reactions in biological membranes [22].

Although there is significant attention on the protective effects of these vitamins individually, limited comparative and combined efficacy data against nanoparticle-induced ovarian injury in particular in terms of the apoptotic signalling axis are available.

The current study thus aimed to investigate whether in a well-controlled rat model of oral ZnO-NP exposure, supplementation with vitamins A, C, or E, individually and in combination, could prevent: (i) ovarian oxidative damage and the depletion of antioxidant enzymes; (ii) histopathological changes in ovaries.

MATERIALS AND METHODS

Chemicals and Nanoparticle Characterization: ZnO-NPs were obtained as uncoated (purity: 99% and primary particle size 30 + 5 nm) and were purchased at Sigma-Aldrich (St. Louis, MO, USA). The morphology of the particles was confirmed by transmission electron microscopy (TEM; JEOL JEM-2100), dynamic light scattering (DLS; Malvern Zetasizer Nano ZS) was used to determine the hydrodynamic diameter and polydispersity index (PDI), and the crystalline phase by X-ray diffraction (XRD; Shimadzu XRD-6100). ZnO-NPs dissolved in deionized water had a mean hydrodynamic

diameter of 95 +/-12 nm, PDI of 0.18 and a zeta potential of -18 +/-2.4 mV. Before every dosing, suspensions were prepared freshly in sterile 0.9% saline, sonicated (100 W, 40 kHz, 30 min, ice bath) and vortexed just before gavage. Retinyl palmitate (vitamin A), L-ascorbic acid (vitamin C), and DL- α -tocopheryl acetate (vitamin E) were obtained from Merck (Darmstadt, Germany).

Animals and Ethical Approval: This study was carried out at the Kut Technical Institute, Middle Technical University, in Al-Kut City, Wasit Province, Iraq — specifically within the Department of Pathological Analysis Techniques and its affiliated animal housing unit. The study protocol and all experimental procedures were reviewed and approved by the Institutional Animal Ethics Committee of the University of Wasit, College of Science (Ethical Approval No. WU-2125), in accordance with national guidelines for the care and use of laboratory animals. The institutional animal house acquired 48 sexually mature Wistar rats (10-12 weeks of age; 180-220 g) and 24 proven fertile males that were housed in a controlled environment (22 o C, 55% relative humidity, 12 h light/dark cycle) with ad libitum access to standard diet and filtered water. All procedures were preceded by a 7-day acclimatisation period. Regular 4–5 day estrous cyclicity was confirmed by vaginal smear cytology for e" two consecutive cycles.

Experimental Design and Dosing: The rats were randomly assigned to six groups of eight and daily dosed by oral gavage over 28 consecutive days (about six estrous cycles). G1 (Control) was treated with sterile saline (1 mL/kg). ZnO-NP suspension (100 mg/kg) was added to G2 (ZnO-NP). G3–G5 received ZnO-NP (100 mg/kg) with vitamin A (1000 IU/kg), vitamin C (200 mg/kg), or vitamin E (100 mg/kg), respectively. G6 was fed with ZnO-NP (100 mg/kg) and A+C+E cocktail in the same doses. Nanoparticles and vitamins were given as two individual gavages with 30 min intervals. The body weight was measured after every three days, and the dosing volumes were changed (Table 1).

Mating Protocol and Preimplantation Embryo Collection: After the last treatment, a proven fertile male (2:1 female-to-male) was cohoused with each female overnight (on the day after the last treatment). Gestational day 0 (GD 0) was determined by vaginal copulatory plug. On GD 5, animals received a dose of sodium pentobarbital (100 mg/kg i.p.) to cause euthanasia. Blood was cardiac punctured; serum was separated (1500 × g, 15 min, 4 0 C) and frozen at -80 C. Both ovaries were excised, trimmed and weighed: the right ovary was snap-frozen (-80 o C) to conduct biochemical analyses, and the left ovary was fixed in 10% neutral-buffered formal PBS-BSA (0.4%) was used to flush the uterus and recover preimplantation embryos and morphologically stage them using stereomicroscopy under x 40 magnification.

Oxidative Stress and Antioxidant Enzyme Assays: Homogenisation of ovarian tissue: Ovarian tissue was homogenised (10% w/v) in ice-cold 50 mM potassium phosphate buffer (pH 7.4) containing 1 mM EDTA and protease inhibitors and centrifuged (10,000 × g, 15 min, 4 o C). The thiobarbituric acid reactive substances (TBARS) technique was used to measure MDA (nmol/mg protein). The Ellman method was used to measure GSH. Pyrogallol autoxidation was used to determine SOD activity and H 2 O 2 decomposition at 240 nm to determine CAT activity. The total protein was measured using the Lowry technique.

Serum Reproductive Hormone Assay:

Validated rat-specific ELISA kits were used to measure serum FSH, LH, 17â-estradiol (E2), and progesterone (P4). All analytes had a coefficient of variation of less than 8% and 12%, respectively, intra-assay and inter-assay.

Histopathological Examination and Follicle Counting (H&E): NBF-fixed ovaries were systematically prepared, embedded in paraffin and serially sectioned at 5 µm. Every fifth section was stained with Harris haematoxylin and eosin (H&E). Follicles were differentiated as primordial, primary, secondary, antral, or atretic based on the well-known morphological features; only those follicles with a visible oocyte nucleus were counted to prevent counting them twice. Two blinded observers agreed on a 0-4 scale (0 = absent, 1 = minimal, 2 = mild, 3 = moderate, 4 = severe)

on the five features: vascular congestion, stromal edema, follicular degeneration, apoptotic bodies and inflammatory infiltration. Weighted kappa was used to assess inter-observer agreement (= 0.88, p < 0.001).

Immunohistochemical Analysis (Bax, Bcl-2, Cleaved Caspase-3): 5 µm paraffin sections were deparaffinized and rehydrated and heat-induced epitope retrieval was performed in 10 mM sodium citrate buffer (pH 6.0, 95 C, 20 min). H 2 O 2/Methanol (3%): 10 min, endogenous peroxidase was quenched. Normal goat serum (10%) was used to block non-specific binding (30 min). Primary antibodies were used overnight at 4 o C: anti-Bax (rabbit polyclonal, 1:200; Abcam ab32503), anti-Bcl-2 (rabbit monoclonal, 1:100; Abcam ab182858) and anti-cleaved caspase-3 (rabbit polyclonal, 1:300; Cell Secondary antibody (HRP-conjugated) (Dako EnVision+) was used (30 min) and DAB chromogen (Dako Liquid DAB+) was used to visualize the immunoreactivity, and then the sample was counterstained with haematoxylin. There was no specific staining of negative controls (no primary antibody was used). The H-score method (ranging 0–300) was used to quantify immunoreactivity in granulosa cells and the percentage of Bax- and Bcl-2-positive cells by colour deconvolution in ImageJ v1.54 (NIH).

TUNEL Assay of In Situ Apoptosis: The DeadEnd Fluorometric TUNEL System (Promega, G3250) was used to detect in situ apoptotic cell death. Samples were permeabilized with proteinase K (20 µg/mL, 8 min), equilibrated and incubated with biotinylated nucleotide/TdT enzyme mixture (37 o C, 60 min, dark). The treatment of slides with streptavidin FITC and DAPI (300 nM) was performed. Positive controls were in the form of DNase I-treated sections. The number of TUNEL-positive (green) and total DAPI (blue) nuclei was counted in at least 10 high-power fields each section (×200, fluorescence microscopy). TUNEL index = (TUNEL positive nuclei/ total DAPI nuclei) x100.

Caspase-3 Enzyme assay: Caspase-3 activity of ovarian homogenate supernatants was determined by colorimetric assay kit (Abcam ab39401) according to the cleavage of Ac-DEVD-pNA substrate at 405 nm after incubation of 2 h at 37 C.

Statistical Analysis:

Data are reported in terms of mean ± SEM (n = 8). The Shapiro-Wilk test was used to test normality and Levene test was used to test variance homogeneity. One-way ANOVA with post-hoc Tukey HSD was used to compare between groups. Inter-observer reliability of histopathological scoring was measured using weighted kappa. Two tailed p < 0.05 was deemed as significant. The IBM SPSS v26 and GraphPad Prism v9 were used to conduct a

Table 1: Experimental groups, designations, and daily oral treatments (n = 8 per group).

Group	Label	Daily Treatment (oral gavage, 28 days)	n
G1	Control	Sterile saline, 1 mL/kg	8
G2	ZnO-NP	ZnO-NP, 100 mg/kg	8
G3	ZnO-NP + Vit A	ZnO-NP (100 mg/kg) + retinyl palmitate (1000 IU/kg)	8
G4	ZnO-NP + Vit C	ZnO-NP (100 mg/kg) + L-ascorbic acid (200 mg/kg)	8
G5	ZnO-NP + Vit E	ZnO-NP (100 mg/kg) + DL-α-tocopheryl acetate (100 mg/kg)	8
G6	ZnO-NP + A+C+E	ZnO-NP (100 mg/kg) + vitamins A (1000 IU/kg) + C (200 mg/kg) + E (100 mg/kg)	8

ZnO-NP, zinc oxide nanoparticle; IU, international units.

RESULTS

General Health, Body Weight, and Ovarian Weight: No mortality or overt signs of toxicity were observed throughout the study. Final body weight gain was significantly reduced in G2 (27.7 ± 3.1 g vs. 54.4 ± 2.3 g in G1; p < 0.05). Absolute ovarian weight was similarly reduced (48.3 ± 2.9 mg vs. 71.8 ± 3.2 mg; p < 0.05).

Vitamin co-administration progressively restored both parameters, with G6 yielding values statistically indistinguishable from controls (Table 2).

Table 2: Body weight parameters and absolute ovarian weight across experimental groups (mean ± SEM, n = 8).

Group	Initial BW (g)	Final BW (g)	BW Gain (g)	Ovarian Wt (mg)
G1 Control	194.2 ± 4.1	248.6 ± 5.8	54.4 ± 2.3	71.8 ± 3.2
G2 ZnO-NP	192.8 ± 3.6	220.5 ± 6.4 *	27.7 ± 3.1 *	48.3 ± 2.9 *
G3 + Vit A	193.6 ± 4.3	234.1 ± 5.6	40.5 ± 2.7 †	58.4 ± 2.7 †
G4 + Vit C	195.1 ± 3.8	236.9 ± 5.2	41.8 ± 2.8 †	60.1 ± 2.5 †
G5 + Vit E	193.0 ± 4.0	239.7 ± 5.9	46.7 ± 2.6 †	63.6 ± 2.8 †
G6 + A+C+E	194.7 ± 3.9	245.3 ± 5.7 †	50.6 ± 2.4 †	68.9 ± 3.0 †‡

** p < 0.05 vs. G1 (Control); † p < 0.05 vs. G2 (ZnO-NP); ‡ p < 0.05 vs. single-vitamin groups (G3–G5).*

Ovarian Oxidative Stress Markers and Antioxidant Enzyme Activities: ZnO-NP administration caused pronounced oxidative imbalance in ovarian tissue (Table 3). MDA nearly tripled in G2 (6.82 ± 0.58 vs. 2.35 ± 0.22 nmol/mg in G1; $p < 0.001$). Concurrently, GSH fell ~61% (11.2 ± 1.3 vs. 28.6 ± 2.1 nmol/mg), SOD activity ~61% (6.9 ± 0.9 vs. 17.8 ± 1.4 U/mg), and CAT ~59% (17.6 ± 2.2 vs. 42.5 ± 3.1 U/mg; all $p < 0.001$). Vitamin co-treatment significantly attenuated these changes, with vitamin E showing greatest individual efficacy for MDA suppression. The combined A+C+E regimen (G6) reduced MDA to 2.78 ± 0.24 nmol/mg and restored GSH, SOD, and CAT activities to 85–93% of control values—significantly surpassing any single vitamin ($p < 0.05$).

Table 3: Ovarian tissue oxidative stress markers and antioxidant enzyme activities (mean ± SEM, n = 8).

Group	MDA (nmol/mg)	GSH (nmol/mg)	SOD (U/mg)	CAT (U/mg)
G1 Control	2.35 ± 0.22	28.6 ± 2.1	17.8 ± 1.4	42.5 ± 3.1
G2 ZnO-NP	6.82 ± 0.58 *	11.2 ± 1.3 *	6.9 ± 0.9 *	17.6 ± 2.2 *
G3 + Vit A	4.05 ± 0.34 †	19.4 ± 1.8 †	11.8 ± 1.1 †	28.4 ± 2.6 †
G4 + Vit C	3.88 ± 0.31 †	20.8 ± 1.9 †	12.6 ± 1.2 †	30.2 ± 2.7 †
G5 + Vit E	3.42 ± 0.28 †	22.7 ± 2.0 †	13.9 ± 1.3 †	33.8 ± 2.9 †
G6 + A+C+E	2.78 ± 0.24 †‡	26.5 ± 2.1 †‡	16.4 ± 1.4 †‡	39.7 ± 3.0 †‡

MDA, malondialdehyde; GSH, reduced glutathione; SOD, superoxide dismutase; CAT, catalase.
* p < 0.001 vs. G1 (Control); † p < 0.05 vs. G2 (ZnO-NP); ‡ p < 0.05 vs. single-vitamin groups.

Serum Reproductive Hormone Profile: ZnO-NP exposure produced a hypergonadotropic–hypogonadal endocrine profile (Table 4). FSH and LH were significantly elevated in G2 (11.4 ± 0.7 and 7.9 ± 0.6 mIU/mL vs. 6.8 ± 0.5 and 4.2 ± 0.4 in G1; $p < 0.01$), while estradiol fell from 48.7 ± 3.2 to 22.6 ± 2.1 pg/mL and progesterone from 22.4 ± 1.8 to 10.8 ± 1.2 ng/mL (both $p < 0.01$). In G6, all four hormone concentrations were statistically indistinguishable from controls ($p > 0.05$; Table 4).

Table 4: Serum reproductive hormone concentrations across experimental groups (mean ± SEM, n = 8).

Group	FSH (mIU/mL)	LH (mIU/mL)	Estradiol (pg/mL)	Progesterone (ng/mL)
G1 Control	6.8 ± 0.5	4.2 ± 0.4	48.7 ± 3.2	22.4 ± 1.8
G2 ZnO-NP	11.4 ± 0.7 *	7.9 ± 0.6 *	22.6 ± 2.1 *	10.8 ± 1.2 *
G3 + Vit A	8.9 ± 0.6 †	5.8 ± 0.5 †	33.8 ± 2.7 †	15.9 ± 1.5 †
G4 + Vit C	8.7 ± 0.6 †	5.6 ± 0.5 †	35.2 ± 2.8 †	16.5 ± 1.5 †
G5 + Vit E	8.2 ± 0.6 †	5.4 ± 0.4 †	37.5 ± 2.9 †	17.8 ± 1.6 †
G6 + A+C+E	7.3 ± 0.5 †‡	4.7 ± 0.4 †‡	44.9 ± 3.1 †‡	20.7 ± 1.7 †‡

FSH, follicle-stimulating hormone; LH, luteinizing hormone. * p < 0.01 vs. G1; † p < 0.05 vs. G2; ‡ p < 0.05 vs. G3–G5.

Ovarian Follicular Counts: Follicular reserve was severely depleted in G2: primordial, primary, secondary, and antral follicle counts were reduced by 50–70% while atretic follicles increased ~four-fold (all $p < 0.001$ vs. G1; Table 5). The combined A+C+E regimen produced the most complete restoration of follicular populations and the greatest reduction in atresia.

Table 5: Mean ovarian follicle counts per representative histological section (mean ± SEM, n = 8).

Group	Primordial	Primary	Secondary	Antral	Atretic
G1 Control	52.3 ± 3.4	28.5 ± 2.1	18.7 ± 1.5	12.4 ± 1.1	4.2 ± 0.5
G2 ZnO-NP	24.8 ± 2.2 *	12.4 ± 1.3 *	7.1 ± 0.9 *	3.8 ± 0.6 *	16.9 ± 1.4 *
G3 + Vit A	36.7 ± 2.6 †	19.8 ± 1.7 †	12.9 ± 1.2 †	7.6 ± 0.8 †	10.4 ± 1.0 †
G4 + Vit C	37.9 ± 2.7 †	20.6 ± 1.7 †	13.4 ± 1.2 †	7.9 ± 0.9 †	9.8 ± 1.0 †
G5 + Vit E	40.5 ± 2.9 †	22.8 ± 1.8 †	14.8 ± 1.3 †	9.1 ± 0.9 †	8.3 ± 0.9 †
G6 + A+C+E	48.1 ± 3.2 †‡	26.3 ± 2.0 †‡	17.2 ± 1.4 †‡	11.0 ± 1.0 †‡	5.4 ± 0.6 †‡

* $p < 0.05$ vs. G1 (Control); † $p < 0.05$ vs. G2 (ZnO-NP); ‡ $p < 0.05$ vs. G3–G5.

Ovarian Histopathological Findings (H&E Staining): Representative photomicrographs of H&E-stained ovarian sections are presented in Figure 1. Detailed histopathological features for each experimental group are described below.

G1 – Control Group: Control ovaries displayed normal cortical and medullary architecture with follicles at all developmental stages present in appropriate proportions. Primordial follicles were abundant in the superficial cortex, identifiable as small structures comprising a large arrested oocyte surrounded by a single layer of flattened pre-granulosa cells. Primary follicles showed a single layer of cuboidal granulosa cells with round, basophilic nuclei. Secondary follicles displayed orderly multilayered granulosa cell arrangements with an early zona pellucida. Antral follicles contained a clearly defined fluid-filled antrum, a compact cumulus oophorus, and well-organised mural granulosa and theca cell layers. Corpora lutea were structurally intact with abundant large, pale, lipid-laden luteal cells and well-developed vasculature. The ovarian stroma showed normal compact fibrovascular organisation. No vascular congestion, edema, inflammatory cell infiltration, pyknotic nuclei, or apoptotic bodies were detected. All semi-quantitative lesion scores were minimal (Table 6).

G2 – ZnO-NP Group (100 mg/kg/day): Ovaries exposed to ZnO-NPs had the most severe and widespread histopathological changes, and the highest overall lesion score (17.1 ± 0.6; Table 6). Cortical and medullary compartments had a high vascular congestion (score 3.5 ± 0.2) with significantly enlarged, full-filled blood vessels and erythrocyte sludging. Extensive interstitial stromal edema (score 3.3 ± 0.2) was present in the form of pale, acellular, fluid filled areas cutting through the stromal matrix. The follicular compartment was highly disturbed: most of the follicles had advanced atretic changes such as pyknotic oocyte nuclei (karyopyknosis and karyorrhexis), disorganised and detached layers of granulosa cells with the loss of intercellular adhesion and focal fragmentation of zona pellucida. The number of atretic follicles was about four times more than the controls. There was a significant loss of primordial follicle reserves. Antral and growing follicles were uncommon and existing follicles had granulosa cell vacuolisation and degenerating oocytes. Apoptotic bodies (score 3.6 ± 0.2) were widely scattered in the follicular granulosa layers and across the stromal interstitium. Perifollicular and medullary areas were found to have focal aggregates of mononuclear inflammatory cells (lymphocytes and macrophages) (score 2.9 ± 0.2). Corpora lutea exhibited signs of premature luteolysis: shrunken, vacuolated, hypereosinophilic, luteal cells with nuclear pyknosis and stromal fibrosis, which is likely reflective of impaired secretion of progesterone.

G3- ZnO-NP + Vitamin A: The recovery was found to be partial (total score 11.1 + 0.5). More of the primordial and primary follicles became identifiable than G2 and there was better follicular cytoarchitecture. Follicular degeneration continued to be moderate, and the number of atretic follicles was still highly increased compared to controls. Vascular congestion, mild to moderate; stromal edema mild to moderate. Compared to G2, the number of apoptotic bodies was reduced. Focal mononuclear inflammatory infiltrates were minimized yet observable.

G4- ZnO-NP + Vitamin C: Histological changes were widely similar to G3 except that it had a slight improvement in granulosa cell layer integrity (total score 10.3 ± 0.5). The secondary follicles had more organised multilayered granulosa arrangements and had fewer pyknotic nuclei. Congestion in the vessel was mild; there was little inflammatory infiltration. There were still scattered apoptotic bodies but at a lower concentration than G2.

G5 ZnO-NP + Vitamin E: The most significant single histological protective effect (overall score 9.0 ± 0.4) was obtained with vitamin E, in accordance with its better ability to suppress MDA. A significantly higher percentage of follicles, especially primordial and primary, was found to be morphologically intact with clearly defined granulosa cell layers and oocyte nuclear morphology. Stromal edema was mild; vascular congestion minimal to mild. There was sparse inflammatory infiltration. Luteal cell morphology was partially restored in corpora lutea.

G6 – ZnO-NP + Combined A+C+E: The integrated vitamin treatment resulted in the best overall histological restoration with an approximation to control ovary morphology (total score 3.3 ± 0.3). All developmental stages of follicles were represented in the normal proportions and morphological features: intact granulosa cell layers, clear oocyte nuclei with strong nucleoli and intact zona pellucida. Stromal tissue was tight and highly structured and there were no substantial edema and only slight vascular congestion. There was no or little inflammatory cell infiltration. Isolated apoptotic bodies were found very infrequently. Corpora lutea were maintained structurally with high lipid-filled luteal cells and normal vascular maintenance indicative of retained progesterone secretory ability.

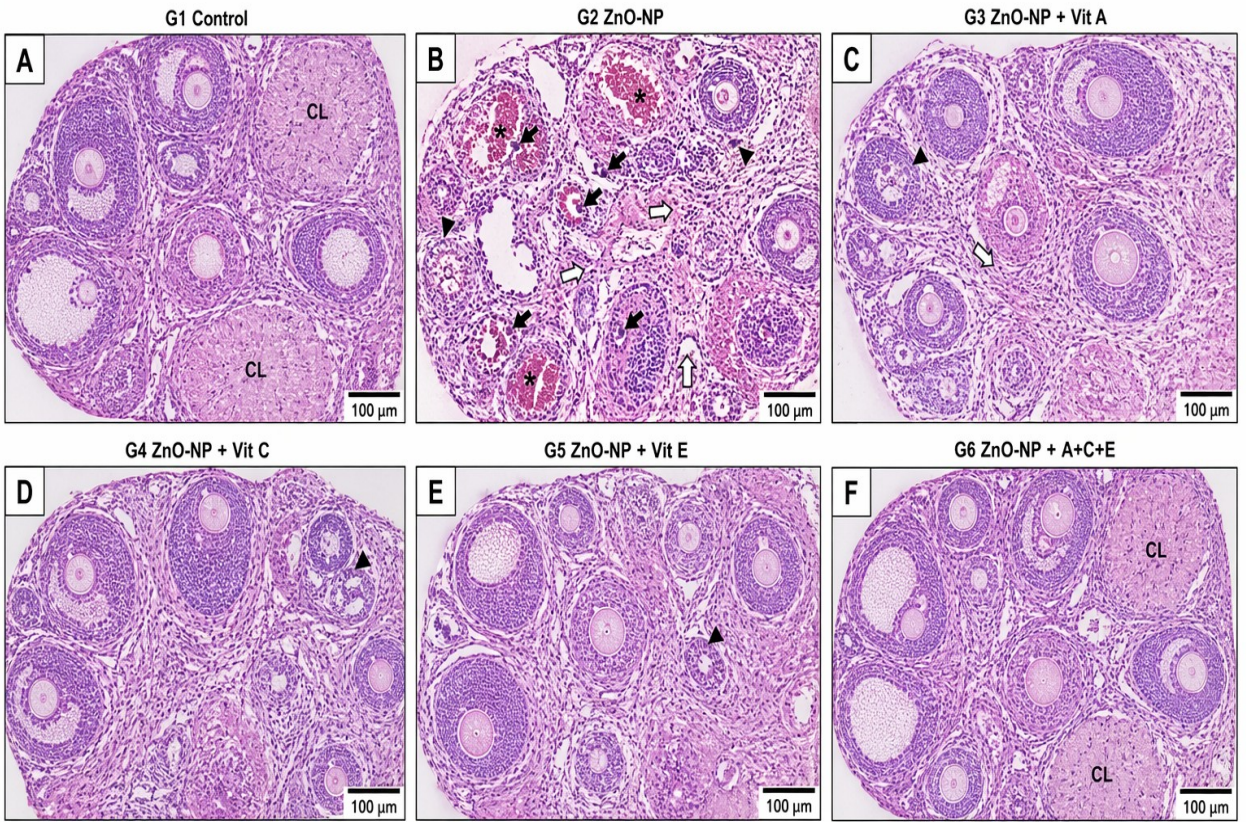

Fig. 1: Representative schematic photomicrographs of ovarian sections stained with haematoxylin and eosin (H&E, ×100). (A) G1 Control: normal architecture—follicles at all stages, intact corpora lutea (*), and organised stroma. (B) G2 ZnO-NP: severe vascular congestion (open arrows), widespread follicular atresia (arrowheads), stromal edema ( ), apoptotic bodies (filled arrows), and inflammatory infiltration. (C–E) G3, G4, G5: progressive histological recovery with decreasing lesion severity. (F) G6 ZnO-NP + A+C+E: near-complete architectural restoration resembling controls. Scale bar = 100 µm.

Table 6: Semi-quantitative histopathological lesion scores (0–4 scale, mean ± SEM, n = 8; inter-observer k = 0.88).

Group	Vascular Congestion	Stromal Edema	Follicular Degeneration	Apoptotic Bodies	Inflammatory Infiltration	Total Score
G1 Control	0.3 ± 0.1	0.2 ± 0.1	0.4 ± 0.1	0.3 ± 0.1	0.2 ± 0.1	1.4 ± 0.3
G2 ZnO-NP	3.5 ± 0.2*	3.3 ± 0.2*	3.8 ± 0.2*	3.6 ± 0.2*	2.9 ± 0.2*	17.1 ± 0.6*
G3 ZnO-NP + Vit A	2.3 ± 0.2†	2.0 ± 0.2†	2.5 ± 0.2†	2.4 ± 0.2†	1.9 ± 0.2†	11.1 ± 0.5†
G4 ZnO-NP + Vit C	2.1 ± 0.2†	1.9 ± 0.2†	2.3 ± 0.2†	2.2 ± 0.2†	1.8 ± 0.2†	10.3 ± 0.5†
G5 ZnO-NP + Vit E	1.8 ± 0.2†	1.7 ± 0.2†	2.0 ± 0.2†	1.9 ± 0.2†	1.6 ± 0.2†	9.0 ± 0.4†
G6 ZnO-NP + A+C+E	0.7 ± 0.1‡	0.6 ± 0.1‡	0.8 ± 0.1‡	0.7 ± 0.1‡	0.5 ± 0.1‡	3.3 ± 0.3‡

* $p < 0.05$ vs. G1 (Control); † $p < 0.05$ vs. G2 (ZnO-NP); ‡ $p < 0.05$ vs. single-vitamin groups

Immunohistochemical Expression of Bax, Bcl-2, and Caspase-3: The Bax immunoreactivity in control ovaries (G1) was low (8.2 ± 1.1% positive granulosa cells), and was limited to atretic follicles, whereas Bcl-2 was strong (78.4 ± 3.2%), revealing mainly an anti-apoptotic signalling in healthy follicles. This yielded a Bax/Bcl-2 ratio of 0.10 ± 0.01. ZnO-NP-treated ovaries (G2) exhibited a dramatic reversal: Bax rose to 72.5 ± 3.8% while Bcl-2 fell to 11.8 ± 1.5%, elevating the Bax/Bcl-2 ratio to 6.14 ± 0.42—a 61-fold increase ($p < 0.001$ vs. G1; Table 8). There was strong cytoplasmic caspase-3 immunoreactivity observed in granulosa layers of degenerating follicles. The restoration of the Bax-low/Bcl-2-high protective profile was progressive, as G3-G5. The A+C+E regimen (G6) reestablished the Bax/Bcl-2 to 0.20 ± 0.02, which is close to control values ($p = 0.28$ vs. G1; Table 7).

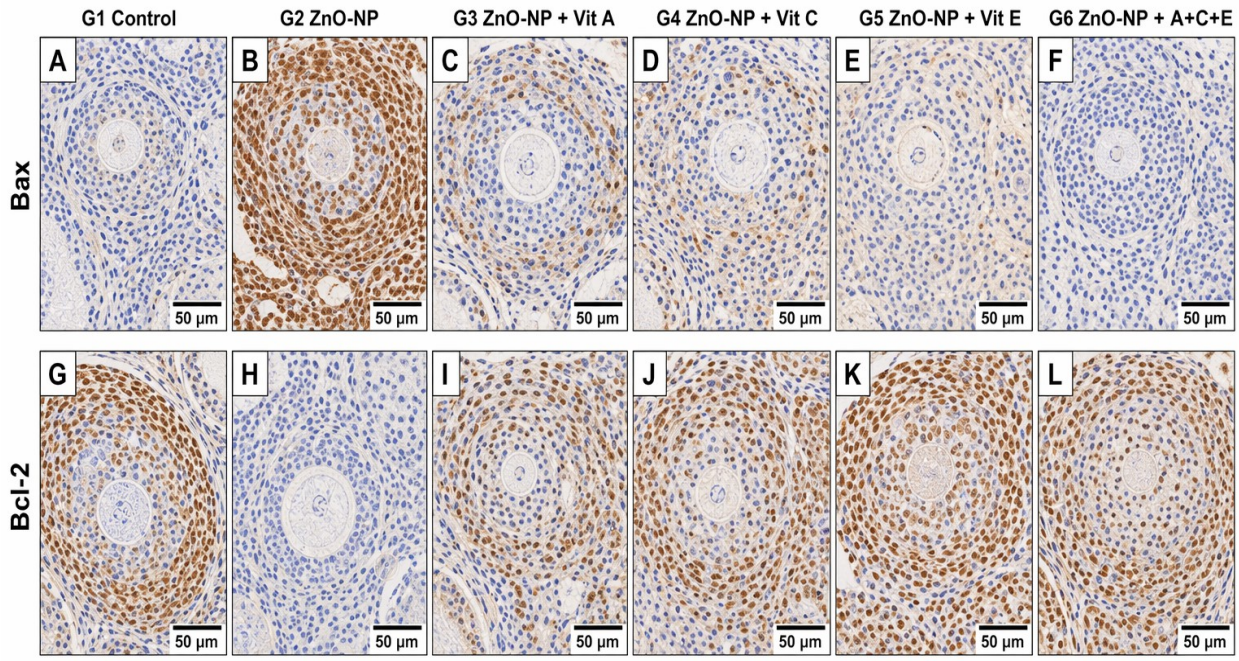

Fig. 2: Immunohistochemical expression of Bax (upper panels, A–F) and Bcl-2 (lower panels, G–L) in ovarian granulosa cells (DAB chromogen/haematoxylin counterstain, ×200). Brown = DAB-positive (protein expressed); blue = haematoxylin counterstain. In G2 (B, H), Bax is strongly and diffusely expressed while Bcl-2 is markedly reduced. Progressive restoration of the Bax-low/Bcl-2-high pattern is evident from G3 to G5, with near-complete reversal in G6 (F, L). Scale bar = 50 µm.

TUNEL Assay and Caspase-3 Enzymatic Activity: The apoptotic cascade was directly confirmed cytologically with the aid of the TUNEL test (Figure 2). Baseline TUNEL index of G1 was 5.2 ± 0.7% and this is physiological granulosa cell apoptosis of atretic follicles. In G2, the abundance of TUNEL-positive nuclei rose rapidly to 67.8 ± 4.1% -13-fold more ($p < 0.001$), including growing and antral follicles that are not normally apoptotic, which is pathologically induced. Individual vitamins reduced the index to 41.5%, 38.2%, and 31.6% for G3, G4, and G5 respectively (all $p < 0.01$ vs. G2). A combination of A + C + E regimen (G6) minimized TUNEL positivity to 10.3 ± 0.9% -85% lower than G2-near control levels ($p = 0.09$ vs. G1).

Caspase-3 activity showed the same pattern: G2 exhibited a 5.2-fold elevation (42.5 ± 3.2 vs. 8.2 ± 0.8 pmol/min/mg protein in G1; $p < 0.001$). The combined vitamin regimen (G6) decreased the activity to 11.4 ± 0.9 pmol/min/mg protein-an 82.7% decrease compared to G2 and statistically the same as controls ($p = 0.12$; Figure 3 G-H; Table 6).

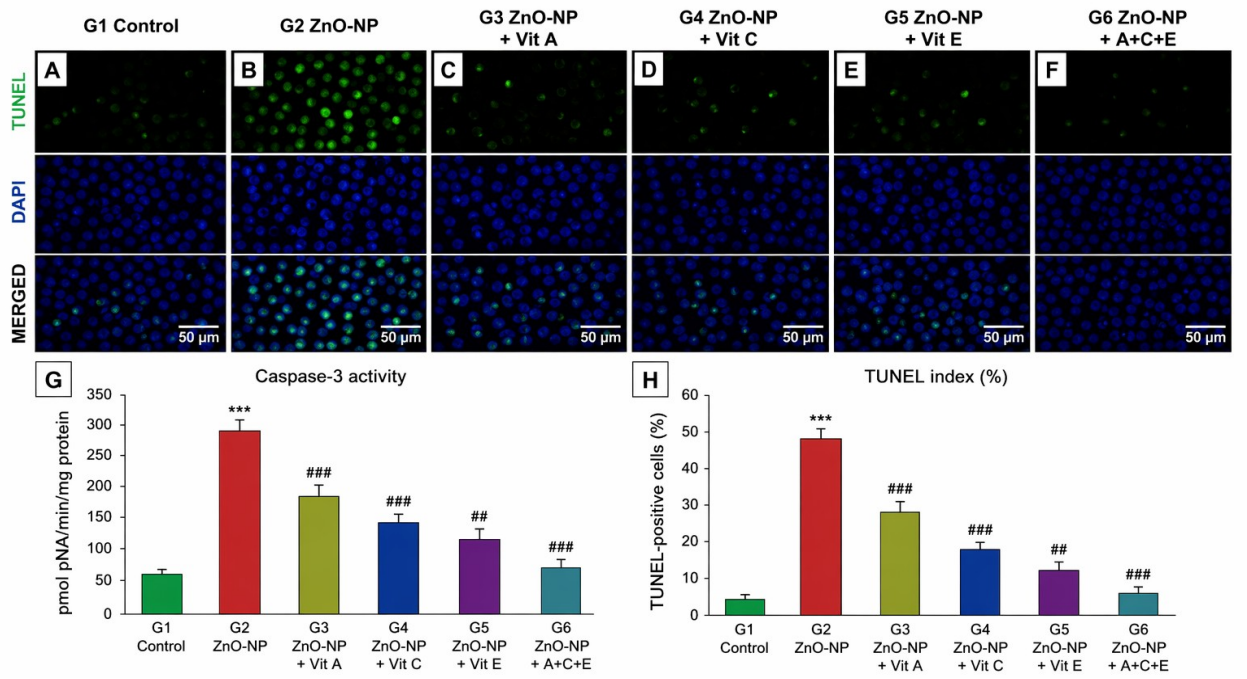

Fig. 3: TUNEL assay and caspase-3 activity. (A–F) Representative fluorescence micrographs across experimental groups (×200): green = TUNEL-positive apoptotic nuclei; blue = DAPI counterstain. Progressive reduction in TUNEL-positive cells from G2 to G6. (G) Caspase-3 enzymatic activity (pmol pNA/min/mg protein). (H) Quantitative TUNEL index (%). Bars = mean ± SEM. *** $p < 0.001$ vs. G1 Control; ## $p < 0.01$, ### $p < 0.001$ vs. G2 ZnO-NP. Scale bar = 50 µm.

Table 7: Immunohistochemical apoptotic markers and caspase-3 enzymatic activity (mean ± SEM, n = 8).

Group	Bax (+%)	Bcl-2 (+%)	Bax/Bcl-2 Ratio	Caspase-3 (pmol/min/mg)	TUNEL Index (%)
G1 Control	8.2 ± 1.1	78.4 ± 3.2	0.10 ± 0.01	8.2 ± 0.8	5.2 ± 0.7
G2 ZnO-NP	72.5 ± 3.8 *	11.8 ± 1.5 *	6.14 ± 0.42 *	42.5 ± 3.2 *	67.8 ± 4.1 *
G3 + Vit A	48.3 ± 2.9 †	38.2 ± 2.8 †	1.26 ± 0.12 †	26.8 ± 2.1 †	41.5 ± 3.0 †
G4 + Vit C	45.1 ± 2.7 †	41.9 ± 2.9 †	1.08 ± 0.10 †	24.5 ± 2.0 †	38.2 ± 2.8 †
G5 + Vit E	38.4 ± 2.5 †	50.3 ± 3.1 †	0.76 ± 0.08 †	20.3 ± 1.8 †	31.6 ± 2.5 †
G6 + A+C+E	14.2 ± 1.5 †‡	72.6 ± 3.2 †‡	0.20 ± 0.02 †‡	11.4 ± 0.9 †‡	10.3 ± 0.9 †‡

* $p < 0.001$ vs. G1 (Control); † $p < 0.05$ vs. G2 (ZnO-NP); ‡ $p < 0.05$ vs. single-vitamin groups (G3–G5).

Table 8: Early embryonic development parameters at gestational day 5 (mean ± SEM, n = 8).

Group	Implantation Rate (%)	Normal Embryos (%)	Mean Blastomere Count (GD 5)
G1 Control	86.4 ± 3.8	91.2 ± 3.1	7.8 ± 0.4
G2 ZnO-NP	42.7 ± 4.2 *	48.6 ± 3.6 *	3.6 ± 0.3 *
G3 + Vit A	63.8 ± 4.0 †	68.4 ± 3.4 †	5.4 ± 0.4 †
G4 + Vit C	66.2 ± 3.9 †	70.7 ± 3.3 †	5.7 ± 0.4 †
G5 + Vit E	69.5 ± 3.9 †	73.5 ± 3.3 †	6.0 ± 0.4 †
G6 + A+C+E	80.3 ± 3.7 †‡	84.7 ± 3.2 †‡	7.1 ± 0.4 †‡

** $p < 0.001$ vs. G1; † $p < 0.05$ vs. G2; ‡ $p < 0.05$ vs. G3–G5.*

Early Embryonic Development Outcomes (GD 5): Embryonic outcomes were consistent with the ovarian findings (Table 6). The mean implantation rate in G2 (42.7 ± 4.2%) was approximately half that of controls (86.4 ± 3.8%; $p < 0.001$). The proportion of morphologically normal preimplantation embryos (48.6 ± 3.6% vs. 91.2 ± 3.1%; $p < 0.001$) and mean blastomere count at GD 5 (3.6 ± 0.3 vs. 7.8 ± 0.4; $p < 0.001$) were similarly reduced, indicating retarded cleavage consistent with compromised oocyte metabolic competence. The combined A+C+E regimen (G6) produced values approaching—but not fully equaling—controls (implantation rate 80.3 ± 3.7%; normal embryos 84.7 ± 3.2%; blastomere count 7.1 ± 0.4; Table 8).

DISCUSSION

Mechanistic Background Oxidative Stress: The significant increase in ovarian MDA (~3-fold) and simultaneous loss of GSH (~61%), SOD (~61%), and CAT (~59%) in G2 indicate that the exposure to ZnO-NPs overwhelms the enzymatic and non-enzymatic antioxidant defenses in the ovaries. This trend is in line with ZnO-NP producing ROS by several convergent pathways: Fenton-like reactions with released Zn 2+ ions; direct electron transfer at the surface of the nanoparticles; disrupting the mitochondrial electron transport chain complexes I and III; and Zn 2+-mediated suppression of thiol-dependent antioxidant enzymes (Nel et al The resultant overproduction of ROS harms the polyunsaturated fatty acids in granulosa cell membranes (producing MDA), drains intracellular GSH, and oxidises SOD and CAT catalytic residues.

The Intrinsic Apoptotic Cascade was activated in Granulosa Cells: The direct proof of the activation of the intrinsic (mitochondrial) apoptotic pathway in ovarian granulosa cells by oxidative injury is demonstrated by the novel IHC and TUNEL data. The 61-fold increase in the Bax/Bcl-2 ratio in G2, accompanied by a 5.2-fold increase in caspase-3 activity, 13-fold increase in TUNEL index, is just the order of events of intrinsic apoptosis: excess ROS increases Bax transcription via p53 activation and PI3K-AKT suppression of survival pathways, and decreases Bcl This Bax/Bcl-2 imbalance facilitates MOMP, cytochrome c release, assembly of Apaf-1 apoptosome, and caspase-9 and caspase-3 activation in a cascade manner [23-25]. ICAD is then cleaved by caspase-3, releasing CAD to induce the internucleosomal DNA fragmentation observed by TUNEL. The fact that TUNEL-positive nuclei were observed in granulosa layers of growing and antral follicles not just in anticipated atretic follicles but also in all ZnO-NP-induced apoptotic induction highlights the pathological nature of its induction.

Follicular and Vascular Injury Evidence by histopathology: These biochemical and molecular events have a morphological correlate, which is given by the detailed histopathological analysis. The vascular congestion and stromal edema in G2 are likely to indicate the presence of microvascular endothelial damage by ZnO-NPs, disrupting oxygen delivery and hormonal signalling to the follicular microenvironment- further increasing the oxidative stress on already damaged granulosa cells due to the direct action of nanoparticles. Inflammatory cell invasion is congruent with the presence of ROS-induced damage-associated molecular patterns (DAMPs) that attract innate immune cells which may create a vicious inflammatory-oxidative loop. The contribution of innate immune signalling cascades, including pattern recognition receptor pathways such as NLRP3 inflammasome activation triggered by damage signals, to sustained tissue-level inflammatory responses has been increasingly recognised across biological systems [26, 27]. The reduced progesterone and diminished endometrial receptivity are directly due to premature luteolysis as indicated by vacuolated, shrunken, and stromal fibrosis-laden luteal cells. The sequential histological recovery G3-G5, with vitamin E offering the most significant protection separately, are consistent with the biochemical oxidative stress measures and confirm the mechanistic relationship between the inhibition of ROS and tissue preservation. Comparable histomorphological alterations in ovarian follicular architecture, including follicular degeneration and stromal disruption, have been independently documented in adult female rats following administration of bioactive compounds, lending further biological credibility to the semi-quantitative scoring approach employed here [28-31].

Embryonic and Hormonal Effects:

Hypergonadotropic-hypogonadal hormonal profile the endocrine consequence of primary ovarian insufficiency after granulosa cell apoptosis and follicular depletion is a direct endocrine consequence of primary ovarian insufficiency in G2. Decreased granulosa cell mass decreases ovarian inhibin B and estradiol, releasing the pituitary from negative feedback and resulting in the increase of FSH and LH a counter-adaptation that is not effective in saving follicular development in the

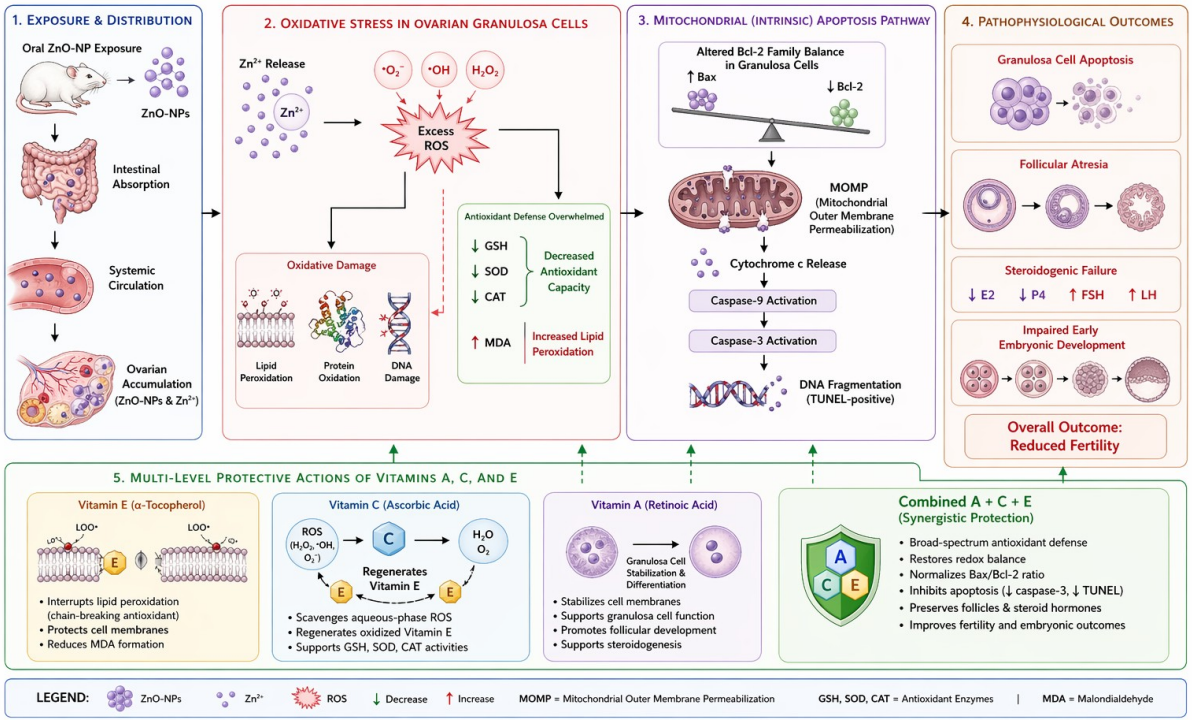

Fig. 4: Proposed mechanistic pathway of ZnO-NP-induced ovarian toxicity and multi-level protective actions of vitamins A, C, and E. Oral ZnO-NP exposure causes systemic Zn^2z release and ovarian nanoparticle accumulation, generating excess ROS. This overwhelms antioxidant defenses (↓GSH, SOD, CAT; ↑ MDA), upregulates Bax and downregulates Bcl-2 in granulosa cells, promoting MOMP, caspase-3 activation, and TUNEL-detectable DNA fragmentation. Progressive granulosa cell apoptosis causes follicular atresia, steroidogenic failure (↓ E2, P4; ↑ FSH, LH), and impaired early embryonic development. Vitamin E interrupts membrane lipid-peroxidation; vitamin C scavenges aqueous-phase ROS and regenerates vitamin E; vitamin A stabilises membranes and supports granulosa cell differentiation. The combined A+C+E regimen provides comprehensive, synergistic protection at all pathway levels.

environment of continued oxidative apoptosis. The recovery of follicular populations in G6 normalised the whole axis of endocrine functions, which supports a causal pathway between follicular integrity and HPG homeostasis. The downstream embryonic losses are indicative of various levels of injury: oxidative DNA and mitochondrial injury in oocytes affects fertilisation and initial cleavage; inhibited progesterone affects endometrial decidualisation and implantation; and disrupted paracrine signalling affects uterine receptivity. The partial recovery of implantation rate in G6 indicates that some of the elements of ZnO-NP damage, possibly epigenetic changes or unremitting oocyte mitochondrial damage, cannot be completely undone by antioxidant treatment in the time interval studied. These observations are consistent with experimental rodent studies demonstrating that pharmacological or hormonal disruption of the follicular axis produces dose-dependent impairment of implantation rate and preimplantation embryo morphology, underscoring the sensitivity of early embryogenesis to follicular microenvironmental insults [32-36].

Combinations of Vitamin Protection and Synergy:

The complementary space and chemical specificities of the three vitamins can be used to justify the superiority of combined A+C+E regimen. The major lipophilic chain-breaking antioxidant in biological membranes is vitamin E (á-tocopherol), which breaks lipid-peroxidation chain reactions by donating a hydrogen atom to peroxyl radicals. Its great ability on a one-on-one basis to suppress MDA and protect histologically is in harmony with membrane-filled granulosa cells being the most important target of the oxidative assault. Vitamin C (ascorbic acid) recycles vitamin E from the tocopheroxyl radical, in a synergistic cycle; it is also a direct scavenger of aqueousphase superoxide, H 2 O 2, and hydroxyl radicals and is concentrated in follicular fluid, placing it best positioned to

neutralise intrafollicular ROS (Padayatty et al., Vitamin A (retinol) plays its role in membrane stabilisation, granulosa cell differentiation regulation through nuclear RARs as well as in steroidogenic enzyme expression-receptor-mediated and differentiation-related aspects of follicular injury that are not responsive to classical antioxidant chemistry [12].

The combination of membrane protection, aqueous-phase scavenging and receptor-mediated signalling is synergistic to explain why the combined regimen is far superior to any single vitamin. Figure 4 shows the proposed mechanistic pathway.

Limitations and Future studies: There are a few shortcomings that should be noted. One dose of ZnO-NP (100 mg/kg/day), particle-size (30 nm) and exposure time (28 days) were tested; future research needs to include dose-response designs with environmentally relevant doses, particle-size studies and ionic zinc controls to separate the effects of particulate vs. Zn 2 +. Molecular characterisation might be further elaborated with upstream ROS sensors (Nrf2/HO-1 pathway), oxidative damage of DNA marker (8-OHdG), ferroptosis-linked pathways (GPX4, SLC7A11), oocyte-specific transcripts (GDF9, BMP15). Additional translational endpoints are pregnancy outcomes (litter size, birth weight, and postnatal development) outside of GD 5. Before translationally applying the vitamin doses used, long-term safety profiling of these doses should also be done.

CONCLUSION

The current research gives a multi-level, mechanistic characterisation of ZnO-NP-induced reproductive toxicity in adult female rats. It is demonstrated that activation of the intrinsic Bax/Bcl-2/caspase-3 apoptotic cascade by oxidative stress in ovarian granulosa cells is one of the core mechanisms underlying follicular atresia, endocrine disruption, and impaired early embryogenesis-supported by convergent biochemical, histopathological, immunohistochemical, TUNEL, and Individual administration of vitamins A, C or E confer partial, but significant protection; the A + C + E regimen, with complementary and synergistic antioxidant effects, gives the most comprehensive restoration across all measured endpoints, nearly to normal ovarian morphology and function. These results suggest that combined antioxidant vitamin supplementation is a promising protective approach to reproductive nanotoxicity and may form the basis of a mechanistic approach to future translational research.

ACKNOWLEDGEMENTS

The authors gratefully acknowledge the technical assistance of the staff of the Animal House Facility, the Central Research Laboratory, and the Department of Histopathology at the Kut Technical Institute, Middle Technical University, particularly for expert support with IHC and TUNEL procedures. This study was conducted in full compliance with institutional and national guidelines for the ethical care and use of experimental animals.

Conflicts of Interests: The authors declare no conflict of interest in relation to the work described in this manuscript.

Ethics Approval: This study was reviewed and approved by the Institutional Animal Ethics Committee of the University of Wasit, College of Science, Iraq (Ethical Approval No. WU-2125). All experimental procedures were carried out at the Kut Technical Institute, Middle Technical University, Al-Kut City, Wasit Province, Iraq, in accordance with national guidelines for the care and use of laboratory animals.

Funding Statement: This research received no specific grant from any funding agency in the public, commercial, or not-for-profit sectors.

Generative Ai Usage Statement:

During the preparation of this manuscript, the authors used a generative AI tool (ChatGPT, OpenAI) solely to improve the language, readability, and clarity of the text. After using this tool, the authors reviewed and edited the content as required and take full responsibility for the content of the publication. No generative AI was used to generate, analyse, or interpret scientific data, results, figures, or conclusions. The authors consent to the display of thisGenerative AI usage statement in the published article.

REFERENCES

[1]. Espitia PJP, Soares NF, Coimbra JS, de Andrade NJ, Cruz RS, Medeiros EA. Zinc oxide nanoparticles: synthesis, antimicrobial activity and food packaging applications. Food Bioprocess Technol 2012;5:1447-1464. https://doi.org/10.1007/s11947-012-0797-6

[2]. Vandebriel RJ, De Jong WH. A review of mammalian toxicity of ZnO nanoparticles. Nanotechnology Science and Applications 2012;5:61-71. https://doi.org/10.2147/NSA.S23932 PMid:24198497 PMCid:PMC3781722

[3]. Tang HQ, Xu M, Rong Q, Jin RW, Liu QJ, Li YL. The effect of ZnO nanoparticles on liver function in rats. Int J Nanomedicine 2016;11:4275-4285. https://doi.org/10.2147/IJN.S109031 PMid:27621621 PMCid:PMC5012617

[4]. Jia J, Li F, Zhou H, Bai Y, Liu S, Jiang Y, et al. Oral exposure to silver nanoparticles or silver ions may aggravate fatty liver disease in overweight mice. Environ Sci Technol 2017;51:9334-9343. https://doi.org/10.1021/acs.est.7b02752 PMid:28723108

[5]. Bhattacharya K, Davoren M, Boertz J, Schins RP, Hoffmann E, Dopp E. Titanium dioxide nanoparticles induce oxidative stress and DNA damage but not DNA-breakage in human lung cells. Part Fibre Toxicol 2009;6:17. https://doi.org/10.1186/1743-8977-6-17 PMid:19545397 PMCid:PMC2711958

[6]. Manke A, Wang L, Rojanasakul Y. Mechanisms of nanoparticle-induced oxidative stress and toxicity. Biomed Res Int 2013;2013:942916. https://doi.org/10.1155/2013/942916 PMid:24027766 PMCid:PMC3762079

[7]. Nel A, Xia T, Mädler L, Li N. Toxic potential of materials at the nanolevel. Science 2006;311:622-627. https://doi.org/10.1126/science.1114397 PMid:16456071

[8]. Agarwal A, Gupta S, Sharma RK. Role of oxidative stress in female reproduction. Reprod Biol Endocrinol 2005;3:28. https://doi.org/10.1186/1477-7827-3-28 PMid:16018814 PMCid:PMC1215514

[9]. Devine PJ, Perreault SD, Luderer U. Roles of reactive oxygen species and antioxidants in ovarian toxicity. Biol Reprod 2012;86:27. https://doi.org/10.1095/biolreprod.111.095224 PMid:22034525 PMCid:PMC3290661

[10]. Luderer U. Ovarian toxicity from reactive oxygen species. Vitam Horm 2014;94:99-127. https://doi.org/10.1016/B978-0-12-800095-3.00004-3 PMid:24388188

[11]. Talebi AR, Khorsandi L, Moridian M. The effect of zinc oxide nanoparticles on mouse spermatogenesis. J Assist Reprod Genet 2013;30:1203-1209. https://doi.org/10.1007/s10815-013-0078-y PMid:23949131 PMCid:PMC3800533

[12]. Tavakoli S, Yari A, Karimi A. Protective effects of vitamin E on reproductive toxicity induced by zinc oxide nanoparticles in female rats. Biol Trace Elem Res 2020;198:508-517.

[13]. Green DR, Llambi F. Cell death signaling. Cold Spring Harb Perspect Biol 2015;7:a006080. https://doi.org/10.1101/cshperspect.a006080 PMid:26626938 PMCid:PMC4665079

[14]. Shu Z, Tian D, Zhang L, Wang Y, Li X, Yang Y. The protective effect of vitamin C on reproductive toxicity induced by ZnO nanoparticles in female mice. Biol Trace Elem Res 2019;191:395-403.

[15]. Zhang H, Ji Z, Xia T, Meng H, Low-Kam C, Liu R, et al. Use of metal oxide nanoparticle band gap to develop a predictive paradigm for oxidative stress and acute pulmonary inflammation. ACS Nano 2012;6:4349-4368. https://doi.org/10.1021/nn3010087 PMid:22502734 PMCid:PMC4139054

[16]. Kim YJ, Kim IT, Park YK, Pyo HM, Ryu H, Kwon D, et al. Zinc oxide nanoparticles induce apoptosis in human endothelial cells. Bull Korean Chem Soc 2006;27:745-751.

[17]. Green DR. Apoptotic pathways: paper wraps stone blunts scissors. Cell 2000;102:1-4. https://doi.org/10.1016/S0092-8674(00)00003-9 PMid:10929706

[18]. Clagett-Dame M, Knutson D. Vitamin A in reproduction and development. Nutrients 2011;3:385-428. https://doi.org/10.3390/nu3040385 PMid:22254103 PMCid:PMC3257687

[19]. Padayatty SJ, Katz A, Wang Y, Eck P, Kwon O, Lee JH, et al. Vitamin C as an antioxidant: evaluation of its role in disease prevention. J Am Coll Nutr 2003;22:18-35. https://doi.org/10.1080/07315724.2003.10719272 PMid:12569111

[20]. Hong JS, Park MK, Kim MS, Lim JH, Park GJ, Maeng EH, et al. Prenatal development toxicity study of zinc oxide nanoparticles in rats. Int J Nanomedicine 2014;9(Suppl 2):159-171. https://doi.org/10.2147/IJN.S57932 PMid:25565834 PMCid:PMC4279776

[21]. Liu J, Zhao Y, Ge W, Zhang P, Liu X, Zhang W, et al. Oocyte exposure to ZnO nanoparticles inhibits early embryonic development through the ã-H2AX and NF-êB signaling pathways. Oncotarget 2017;8:42673-42692. https://doi.org/10.18632/oncotarget.17349 PMid:28487501 PMCid:PMC5522097

[22]. Traber MG, Atkinson J. Vitamin E, antioxidant and nothing more. Free Radic Biol Med 2007;43:4-15. https://doi.org/10.1016/j.freeradbiomed.2007.03.024 PMid:17561088 PMCid:PMC2040110

[23]. Cai J, Yang J, Jones DP. Mitochondrial control of apoptosis: the role of cytochrome c. Biochim Biophys Acta 1998;1366:139-149. https://doi.org/10.1016/S0005-2728(98)00109-1 PMid:9714780

[24]. Sharma V, Singh P, Pandey AK, Dhawan A. Induction of oxidative stress, DNA damage and apoptosis in mouse liver after sub-acute oral exposure to zinc oxide nanoparticles. Mutat Res 2012;745:84-91. https://doi.org/10.1016/j.mrgentox.2011.12.009 PMid:22198329

[25]. Shahin NN, Mohamed MM. Nano-sized titanium dioxide toxicity in rat prostate and testis: ameliorative effect of morin. Toxicol Appl Pharmacol 2017;334:129-141. https://doi.org/10.1016/j.taap.2017.08.014 PMid:28844848

[26]. Al-Ogaili AS, Hameed SS, Noori N. LPS-induced NLRP3 gene expression in chicken. Open Vet J 2022;12(2):197-203. https://doi.org/10.5455/OVJ.2022.v12.i2.7 PMid:35603067 PMCid:PMC9109847

[27]. Radad K, Al-Shraim M, Moldzio R, Rausch WD. Recent advances in benefits and hazards of engineered nanoparticles. Environ Toxicol Pharmacol 2014;37:578-588.

[28]. Hussain MJ, Sarboot AK, Hussein EF. Histological study of celery aqueous seeds extract (Apium graveolens L.) on ovaries in adult female rats. Plant Archives 2018;18(2):2717-2722.

[29]. Abid Al-Shemary NN, Mousa SA, Muslim ZZ. Histological and hormonal study about the effect of aqueous extract of Ocimum gratissimum on female reproductive system in albino mice. J Pharm Sci Res 2018;10(4):765-767.

[30]. Oberdörster G, Oberdörster E, Oberdörster J. Nanotoxicology: an emerging discipline evolving from studies of ultrafine particles. Environ Health Perspect 2005;113:823-839. https://doi.org/10.1289/ehp.7339 PMid:16002369 PMCid:PMC1257642

[31]. Porter AG, Jänicke RU. Emerging roles of caspase-3 in apoptosis. Cell Death Differ 1999;6:99-104. https://doi.org/10.1038/sj.cdd.4400476 PMid:10200555

[32]. AL-Rikabi SAM, Al Shemary NNA. The effect of letrozole treatment on the fertility and embryos parameters in female mice: Histological and hormonal study. J Pak Med Assoc 2023;73(9):S150-S154. https://doi.org/10.47391/JPMA.IQ-31

[33]. AL-Rekabi SAM, Talib Abed W, Al-shemary NNA. Impact of aspirin suppositories on fertility in female mice. Indian J Forensic Med Toxicol 2019;13(4):1505-1509. https://doi.org/10.5958/0973-9130.2019.00515.2

[34]. Abed WT, Mousa SA. Detection of anti-rubella IgM, IgG and antisperm antibodies in the sera of aborted and non-pregnant women in the Kirkuk City. Indian J Forensic Med Toxicol 2019;13(4):1510-1515. https://doi.org/10.5958/0973-9130.2019.00516.4

[35]. Abbasalipourkabir R, Moradi H, Zarei S, Asadi S, Salehzadeh A, Ghafourikhosroshahi A, et al. Toxicity of zinc oxide nanoparticles on adult male Wistar rats. Food Chem Toxicol 2015;84:154-160. https://doi.org/10.1016/j.fct.2015.08.019 PMid:26316185

[36]. Almansour MI, Alferah MA, Shraideh ZA, Jarrar BM. Zinc oxide nanoparticles hepatotoxicity: histological and histochemical study. Environ Toxicol Pharmacol 2017;51:124-130. https://doi.org/10.1016/j.etap.2017.02.015 PMid:28236584

How to cite this article: Sally Adnan Mousa Al-Rikabi Protective Effects of Vitamins A, C, and E on Ovarian Histopathology, Apoptotic Signaling, Oxidative Stress, and Early Embryonic Development in Zinc Oxide Nanoparticle-Induced Toxicity in Female Rats. Int J Anat Res 2026;14(3):9622-9635. **DOI:** 10.16965/ijar.2026.178